

# Preference-Guided Reinforcement Learning for Efficient Exploration

Guojian Wang, Faguo Wu, Xiao Zhang, Tianyuan Chen, Xuyang Chen,  
and Lin Zhao *Member, IEEE*

**Abstract**—In this paper, we investigate preference-based reinforcement learning (PbRL) that allows reinforcement learning (RL) agents to learn from human feedback. This is particularly valuable when defining a fine-grain reward function is not feasible. However, this approach is inefficient and impractical for promoting deep exploration in hard-exploration tasks with long horizons and sparse rewards. To tackle this issue, we introduce LOPE: Learning Online with trajectory Preference guidanceE, an end-to-end preference-guided RL framework that enhances exploration efficiency in hard-exploration tasks. Our intuition is that LOPE directly adjusts the focus of online exploration by considering human feedback as guidance, avoiding learning a separate reward model from preferences. Specifically, LOPE includes a two-step sequential policy optimization process consisting of trust-region-based policy improvement and preference guidance steps. We reformulate preference guidance as a novel trajectory-wise state marginal matching problem that minimizes the maximum mean discrepancy distance between the preferred trajectories and the learned policy. Furthermore, we provide a theoretical analysis to characterize the performance improvement bound and evaluate the LOPE’s effectiveness. When assessed in various challenging hard-exploration environments, LOPE outperforms several state-of-the-art methods regarding convergence rate and overall performance. The code used in this study is available at <https://github.com/buaawgj/LOPE>.

**Index Terms**—Deep reinforcement learning, hard exploration, trajectory preference, state marginal matching, two-step policy optimization.

## I. INTRODUCTION

**D**EEP reinforcement learning (DRL) has recently successfully solved challenging problems through trial and error [1]–[3]. However, many real-world tasks involve long horizons and poorly defined goals and specifying a suitable

reward function in these tasks is difficult [4], [5]. Such hard-exploration tasks remain exceedingly challenging for DRL [6], [7]. It is difficult for agents to explore efficiently and obtain highly rewarded trajectories in such environments [6]. This realistic problem further imposes an extreme urgency for efficient exploration, and overcoming this drawback can considerably expand the possible impact of RL.

An alternative to mitigate the sparsity of reward feedback is preference-based reinforcement learning (PbRL) [8], [9]. In PbRL, instead of directly receiving the instant reward information on each encountered state-action pair, the agent only obtains 1-bit preference feedback for each state-action pair or trajectory from a human overseer [10], [11]. To acquire a dense reward function, many prior PbRL methods employ specialized models to learn separate reward functions from human preferences and then train policies using these learned reward functions [12], [13]. Such a method suggests that the agent is instructed to act optimally indirectly. Furthermore, it increases model complexity and inexplainsability and creates a potential information bottleneck.

Most existing PbRL approaches do not consider scaling to hard-exploration tasks [11], [13]. Although learning a separate reward function does help in solving the sparse reward problem, continuously enforcing such preference-based rewards during the whole training phase cannot guarantee deep exploration in hard-exploration tasks. Only a few studies encourage exploration based on uncertainty in learned reward functions for PbRL algorithms [14]. However, we have no guarantee of achieving deep exploration with this method in hard-exploration tasks with long horizons and large state spaces. Therefore, scaling PbRL to hard-exploration tasks can fill this research gap of RL.

In this study, we propose a novel online RL algorithm called **Learning Online with trajectory Preference guidanceE (LOPE)**, an end-to-end framework that jointly encourages exploration and learns the optimal control policy by regarding human preferences as guidance. Our intuition is that LOPE orients its policy according to human preferences and fully utilizes the distribution information of preferences. LOPE involves a two-step sequential policy optimization process, including trust-region-based policy improvement and preference guidance steps. Specifically, the first step is to employ a trust-region-based approach to generate a candidate policy. In the second step, we introduce a novel trajectory-based distance between policies based on the maximum mean discrepancy (MMD) and reformulate preference guidance as a novel trajectory-wise state marginal matching problem. We then show this

Manuscript received June 14, 2024.

Xiao Zhang and Faguo Wu are the corresponding authors (e-mail: xiao.zh@buaa.edu.cn, faguo@buaa.edu.cn).

Guojian Wang, Xiao Zhang are with the School of Mathematical Sciences, Beihang University, Beijing 100191, China, and with the Key Laboratory of Mathematics, Informatics, and Behavioral Semantics, Ministry of Education, Beijing 100191, China, and also Beijing Advanced Innovation Center for Future Blockchain and Privacy Computing, Beijing 100191, China. Xiao Zhang is also with Zhongguancun Laboratory, Beijing 100194, China (e-mails: wgj@buaa.edu.cn and xiao.zh@buaa.edu.cn).

Faguo Wu and Tianyuan Chen are with the Institute of Artificial Intelligence, Beihang University, Beijing 100191, China, and with the Key Laboratory of Mathematics, Informatics, and Behavioral Semantics, Ministry of Education, Beijing 100191, China, and with Beijing Advanced Innovation Center for Future Blockchain and Privacy Computing, Beijing 100191, China, and also with Zhongguancun Laboratory, Beijing 100194, China (e-mails: faguo@buaa.edu.cn and ctymath@buaa.edu.cn).

Xuyang Chen and Lin Zhao are with the Department of Electrical and Computer Engineering, National University of Singapore, Singapore 117583 (e-mails: chenxuyang@u.nus.edu and elezhli@nus.edu.sg).

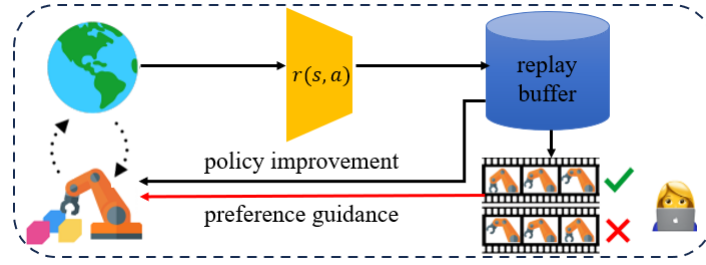


Fig. 1. Illustration of our method. First, the agent interacts with the environment by the policy  $\pi$  and collects a set  $\mathcal{B}$  of trajectories  $\{\tau^1, \dots, \tau^K\}$ . Then, we calculate the policy gradient based on environmental rewards and update policy parameters to increase the expected return and update the current policy toward human preferences. We send the set of trajectories  $\mathcal{B}$  to the annotator for a comparison with trajectories in the preferred-trajectory set  $\mathcal{P}$  and update  $\mathcal{P}$ .

trajectory-wise state marginal matching problem can be transformed into a policy-gradient algorithm with shaped rewards learned from human preferences. Furthermore, this approach enables us to provide theoretical performance guarantees for performance improvement while achieving outstanding performance in various benchmark tasks. Extensive experimental results illustrate the superior performance of LOPE against competitive baselines.

Our contributions are summarized as follows: (1) LOPE: a simple, efficient, and end-to-end PbRL approach that addresses the exploration difficulty by regarding human preferences as guidance; (2) a novel preference-guided trajectory-wise state marginal matching optimization objective and a two-step optimization framework; (3) no requirement for additional neural networks; (4) analytical performance guarantees of LOPE.

The remainder of this paper is organized as follows. Section II introduces recent impressive studies of relevant areas. Section III briefly describes the important background knowledge. Then, Section IV introduces the LOPE approach in detail. Section V analyzes the performance improvement bound of LOPE. The experimental setups are presented in Section VI. Section VII presents the experimental results of LOPE. Finally, Section VIII summarizes the main conclusion of this study.

## II. RELATED WORK

### A. Preference-based RL

Preference-based RL is viewed as human-in-the-loop reinforcement learning by learning from human feedback [15]. Overall, there are three main types of preference feedback in the recent PbRL work. The first category of human preference indicates the preferred states between different state pairs, where actions that are better than all available actions exist in the other state [15]. Second, action preferences are defined on the action space to determine the better action in a given state [8], [16]–[19]. Lastly, trajectory preferences compare the human feedback between trajectory pairs and specify the preferred trajectories over the other ones [10], [12].

Trajectory preferences are the most popular form among the three types of human feedback and are the main focus of many researches [11]. Recently, some impressive work introduced some theoretical results about PbRL with trajectory feedback, which mainly concentrate on the tabular RL setting [20]–[22]. [11] propose an end-to-end offline preference-guided RL

algorithm to avoid the potential information bottleneck. SURF infers the pseudo-labels of unlabeled samples based on the confidence of the preference predictor for reward learning [23]. However, these approaches often require learning a separate reward function corresponding to human feedback or an extra model to encode preference information, causing a higher computation burden and unstable training.

### B. Learn from Demonstrations (LfD)

The objective of LfD is to improve the policy exploration ability of the agent and accelerate learning using the combination of RL with expert demonstration experience [24]. Recently, various work has focused on the research field of LfD. [25] uses expert demonstrations to design an auxiliary margin loss for a pre-trained deep Q-function. [26] shows that model-free DRL algorithms can scale to high-dimensional dexterous manipulation by behavior cloning from a few human expert demonstrations. AWAC accelerates learning of online RL by leveraging a prodigious amount of offline demonstration data with associated rewards [27]. LOGO exploits offline and imperfect demonstrations generated by a sub-optimal policy to achieve faster and more efficient online RL policy optimization [28]. Self-imitation learning (SIL) methods train the agent to imitate its past self-generated experience only when the return of the trajectory exceeds the value function of a certain threshold [29]–[31]. However, LfD methods place a high demand on high-quality demonstrations, and the performance of these methods is limited by the expert policy that generated the demonstration data.

### C. RL with Once-per-episode Feedback

The goal of RL with once-per-episode feedback is to design a new paradigm to cope with the lack of reward functions in various realistic scenarios in which a reward is only revealed at the end of the episode. [32] propose to use an online linear bandit algorithm [33] to directly estimate the underlying Markov reward function and introduce a hybrid optimistic-Thompson Sampling method with a  $\sqrt{K}$  regret. Meanwhile, [34] abandon the Markov reward assumption to provide an efficient algorithm based on the recent work [35], obtaining its regret bounds with the UCBVI algorithm [36]. [37] propose the PARTED algorithm that decomposes the trajectory-wise return into a reward sequence for every state-action pair in

the trajectory and then performs a pessimistic value function update using the learned rewards. Unlike this, our method exploits human feedback to guide agents to explore environments efficiently and can be applied to more complicated scenes.

### III. PRELIMINARIES

#### A. Reinforcement Learning

We formulate the reinforcement learning problem as a discrete-time Markov decision process (MDP) [38] described by a tuple  $(\mathcal{S}, \mathcal{A}, r, P, \rho_0, \gamma)$ . Here,  $\mathcal{S}$  and  $\mathcal{A}$  denote the spaces of states and actions, respectively.  $\gamma \in (0, 1)$  is the discount factor. A stochastic policy  $\pi(a_t|s_t)$  defines an action probability distribution conditioned by  $s_t$ . At each time step  $t$ , given an action  $a_t$  from  $\pi$ , the agent samples the next state  $s_{t+1}$  from the transition probability distribution  $P$ , i.e.,  $s_{t+1} \sim P(s_{t+1}|s_t, a_t)$ , and it receives a reward  $r(s_t, a_t)$  determined by the reward function  $r : \mathcal{S} \times \mathcal{A} \rightarrow \mathbb{R}$ .  $\rho_0$  is the initial state distribution. The objective function is expressed as the expectation of discounted cumulative rewards:

$$J(\pi) = \mathbb{E}_{\tau \sim \pi} [R(\tau)]. \quad (1)$$

Here,  $\tau$  denotes a trajectory  $\{s_0, a_0, s_1, a_1, \dots\}$ ,  $R(\tau)$  is the sum of the discounted cumulative rewards over  $\tau$ ,  $R(\tau) = \sum_{k=0}^{\infty} \gamma^k r(s_{t+k}, a_{t+k})$ . When  $\gamma < 1$ , a discounted state visitation distribution  $d_\pi$  can be given as:  $d_\pi(s) = (1 - \gamma) \sum_{t=0}^{\infty} \gamma^t \mathbb{P}(s_t = s|\pi)$ , where  $\mathbb{P}(s_t = s|\pi)$  denotes the probability of  $s_t = s$  with respect to the randomness induced by  $\pi$ ,  $P$  and  $\rho_0$ .

#### B. PbRL with Trajectory Preferences

In this study, we consider a PbRL framework with trajectory preferences. Unlike the standard RL problem setting, where the agent can receive per-step proxy rewards, we do not assume such instantaneous rewards are accessible. Instead, the agent can only obtain trajectory preferences revealed by an annotator during the early training process. Given these trajectory preferences, suppose that there is a reward function  $r_\psi(s_t, a_t)$  that coincides with these human preferences, the goal of PbRL algorithms is to learn a policy  $\pi(a_t|s_t)$  to maximize the expected (discounted) cumulative rewards  $J_{r_\psi}$ . To achieve this goal, vast amounts of previous work learn a reward function with these human preferences [12], [39]–[41], which is supposed to be consistent with the expert preferences. In contrast, our method directly the policy from these trajectory preferences.

#### C. State Marginal Matching

State marginal matching (SMM) has been recently studied as an alternative problem in RL [42]–[44]. Different from the RL objective to maximize the expected return, the SMM objective is to find a policy whose state marginal distribution  $\rho_\pi(s)$  minimizes the divergence  $D$  to a given target distribution  $\rho^*(s)$ :

$$\mathcal{L}_{\text{SMM}}(\pi) = -D(\rho_\pi(s), \rho^*(s)), \quad (2)$$

where  $D$  is a divergence measure such as Kullback-Leibler (KL) divergence [42] and Jensen-Shannon (JS) divergence [45]. For the target distribution  $\rho^*(s)$ , [42] utilize a uniform distribution to improve exploration in the entire state space; some other approaches leverage imitation learning to match a small set of expert demonstrations [43], [45], [46].

#### D. Maximum Mean Discrepancy

The maximum mean discrepancy (MMD) is an integral probability metric that can be used to measure the difference (or similarity) between two different probability distributions [47]–[49]. Suppose that  $p$  and  $q$  are the probability distributions defined on a nonempty compact metric space  $\mathbb{X}$ . Let  $x$  and  $y$  be observations sampled independently from  $p$  and  $q$ , respectively. Given a Reproducing Kernel Hilbert Space (RKHS)  $\mathcal{H}$ , the MMD metric is given as:

$$\text{MMD}^2(p, q, \mathcal{H}) = \mathbb{E}[k(x, x')] - 2\mathbb{E}[k(x, y)] + \mathbb{E}[k(y, y')], \quad (3)$$

where  $x, x'$  i.i.d.  $\sim p$  and  $y, y'$  i.i.d.  $\sim q$ . Eq. (3) is tractable to estimate the MMD distance between  $p$  and  $q$  using finite samples because  $\mathcal{H}$  only has a kernel function.

### IV. LEARNING ONLINE WITH TRAJECTORY PREFERENCE GUIDANCE

This section presents a novel online PbRL algorithm called **Learning Online with trajectory Preference guidance (LOPE)**. Our main idea is to consider trajectory preferences as guidance for direct policy optimization in hard-exploration tasks, avoiding the potential information bottleneck incurred by learning separate reward functions from these preferences. We first introduce a novel preference-guided trajectory-wise state marginal matching optimization objective by reformulating a constrained optimization problem. Then, we develop a two-step policy optimization framework by integrating a policy improvement step with an additional preference guidance step.

At every point in time, our method maintains a control policy  $\pi : \mathcal{S} \rightarrow \mathcal{A}$  parameterized by deep neural networks, and this policy is updated by the following three processes:

- 1) The agent interacts with the environment by the policy  $\pi$  and collects a set  $\mathcal{B}$  of trajectories  $\{\tau^1, \dots, \tau^K\}$ .
- 2) Policy improvement (PI): We calculate the policy gradient based on environmental rewards and update policy parameters to increase the expected return.
- 3) Preference guidance (PG): We compute the preference-guided gradient and update the current policy toward human preferences.
- 4) The agent sends the set of trajectories  $\mathcal{B}$  to the annotator for a comparison with trajectories in the preferred-trajectory set  $\mathcal{P}$  and updates  $\mathcal{P}$ .

#### A. Human-in-loop: Trajectory-Wise State Marginal Matching

Many previous works of PbRL explicitly learn reward functions coinciding with human preferences. Alternatively, we seek to perform direct policy optimization with a preference-labeled data set. Inspired by previous research [42], [43], we propose reforming preference guidance as a trajectory-wise

state marginal matching problem. Specifically, we define the divergence  $d(\tau, v)$  between state visitation distributions of trajectories  $\tau$  and  $v$ . Then, based on  $d(\cdot, \cdot)$ , we obtain the following trajectory-wise state marginal matching objective between  $\pi$  and  $\pi_b$ :

$$\mathcal{L}_{\text{TW}}(\theta) = \mathbb{E}_{\tau \sim \rho_\theta} \left[ \mathbb{E}_{v \sim \mathcal{P}} [d(\tau, v)] \right], \quad (4)$$

where  $\rho_\theta$  is a distribution induced by  $\pi_\theta$  over the trajectory space.

Compared with previous studies of state marginal matching [42], [43], our approach emphasizes trajectory-level alignment. During training, many state-action pairs are concentrated near the starting point, and only on rare occasions can the agent visit novel regions. Hence, due to the low data proportion, these novel state-action pairs have little impact on policy optimization when the SMM objective only considers the divergence between different state visitation distributions. Our approach solves this problem by introducing a trajectory-wise SMM objective and drives the agent to achieve deep exploration.

Now the focus of the problem comes to the definition of  $d(\cdot, \cdot)$ . Inspired by previous research [48], [50], a trajectory can be considered a deterministic policy, and the distance between them can be defined as the MMD between their state visitation distributions. Therefore,  $d(\cdot, \cdot)$  can be expressed as:

$$\begin{aligned} d(\tau, v) = & \mathbb{E}_{s_\tau, s'_\tau \sim \rho_\tau} [k(s_\tau, s'_\tau)] - 2 \mathbb{E}_{\substack{s_\tau \sim \rho_\tau \\ s_v \sim \rho_v}} [k(s_\tau, s_v)] \\ & + \mathbb{E}_{s_v, s'_v \sim \rho_v} [k(s_v, s'_v)], \end{aligned} \quad (5)$$

where  $\rho_\tau$  and  $\rho_v$  are the state visitation distributions of  $\tau$  and  $v$ . To guarantee the stability of policy optimization, we further adopt the trust-region-based optimization method similar to TRPO [51]:

$$\begin{aligned} \pi_{\text{new}} = & \arg \min_{\pi_\theta} \mathcal{L}_{\text{TW}}(\theta) \\ \text{s.t. } & D_{\text{KL}}(\pi_\theta, \pi_{\text{old}}) \leq \delta. \end{aligned} \quad (6)$$

Intuitively, this preference-guided objective function aids learning by orienting the agent's policy toward human feedback. Specifically, our approach finds a new policy  $\pi_{\text{new}}$  that minimizes the expected trajectory-wise MMD distance to  $\pi_b$ , while ensuring  $\pi_{\text{new}}$  to lie inside the trust region around  $\pi_{\text{old}}$ . This preference-guided policy optimization is the key distinguishing LOPE from other PbRL approaches. This method equips LOPE with two unique advantages over other state-of-the-art algorithms.

First, many previous PbRL studies explicitly learn separate reward functions and then employ off-the-shelf RL algorithms to train a control policy. In contrast, LOPE considers preference-labeled trajectories as guidance and reformulates a novel constrained optimization problem in Eq. (6). In this manner, LOPE effectively avoids the potential information bottleneck incurred by conveying information from preferences to the policy via the scalar rewards.

Second, LOPE learns a policy matching the trajectory-wise state visitation distribution of preference-labeled experiences. Consequently, LOPE enables the agent to quickly expand the

scope of exploration along the preference-labeled trajectories in  $\mathcal{P}$  and overcome the challenging exploration difficulty in online RL settings. Fundamentally, the proposed approach allows us to explore the available information of preference data more comprehensively, such as position information, allowing more significant assistance to RL algorithms.

## B. Two-step Policy Optimization Framework

This section presents a two-step policy optimization framework to provide exploration aid and accelerate learning for the agent. Formally, the policy  $\pi_\theta$  is updated by the following process:

### Step 1: Policy Improvement

LOPE performs one-step policy improvement by optimizing the standard trust-region-based objective function [51]. This can be expressed as follows:

$$\begin{aligned} \pi_{k+\frac{1}{2}} = & \arg \max_{\pi_\theta} \mathbb{E}_{\substack{s \sim d_k \\ a \sim \pi_\theta}} [A_k(s, a)], \\ \text{s.t. } & D_{\text{KL}}(\pi_\theta, \pi_k) \leq \delta. \end{aligned} \quad (7)$$

Here,  $d_k$  is the discounted state visitation distribution corresponding to  $\pi_k$ , and  $A_k(s, a)$  is the advantage of  $\pi_k$  in the state-action pair  $(s, a)$ . The trust-region-based update in Eq. (7) is to find a new policy  $\pi_{k+\frac{1}{2}}$  that maximizes the RL objective while ensuring this new policy stays within the trust region around  $\pi_k$ . From an implementation perspective, off-the-shelf algorithms can solve this optimization problem, such as TRPO [51] or PPO [52].

### Step 2: Preference Guidance

Many RL approaches achieve efficient online policy optimization in dense reward settings. Nonetheless, they may often fail due to the sparsity of reward functions. It is a forlorn hope to achieve significant performance improvement with sparse-reward feedback in the initial training stage. We propose to overcome this difficulty of exploration by using preference as guidance and adjusting policy optimization directly. The preference guidance step is given as follows:

$$\begin{aligned} \pi_{k+1} = & \arg \min_{\pi_\theta} \mathbb{E}_{\tau \sim \rho_\theta} \left[ \mathbb{E}_{v \sim \mathcal{P}} [d(\tau, v)] \right], \\ \text{s.t. } & D_{\text{KL}}(\pi_\theta, \pi_{k+\frac{1}{2}}) \leq \delta. \end{aligned} \quad (8)$$

This preference guidance step is derived from Eq. (6). We solve Eq. (8) by introducing a novel policy gradient. Instead of directly computing the gradient update direction to maximize Eq. (8) as [48], we seek to solve an equivalent optimization problem, which is obtained by expanding the objective function in Eq. (8). This divergence minimization problem can be reduced into a policy-gradient algorithm with shaped rewards computed from  $\mathcal{P}$ .

**Lemma 1** (Preference guidance). *Let  $r_g(s, a)$  denote the preference guidance-based rewards, and it is expressed as:*

$$r_g(s, a) = \mathbb{E}_{\tau \in \mathcal{P}_{s,a}} [\text{dist}(\tau, \mathcal{P})]. \quad (9)$$

Here,  $\text{dist}(\tau, \mathcal{P})$  is considered the distance between  $\tau$  and  $\mathcal{P}$ , i.e.  $\text{dist}(\tau, \mathcal{P}) = \mathbb{E}_{v \sim \mathcal{P}} [d(\tau, v)]$ , and  $\mathcal{P}_{s,a} = \{\tau \in \mathcal{P} | (s, a) \in \tau\}$ . Then, Eq. (8) can be expanded as follows:

$$\begin{aligned} \pi_{k+1} &= \arg \min_{\pi_\theta} \mathbb{E}_{\substack{s \sim d_\theta \\ a \sim \pi_\theta}} [r_g(s, a)], \\ \text{s.t. } D_{\text{KL}}(\pi_\theta, \pi_{k+\frac{1}{2}}) &\leq \delta. \end{aligned} \quad (10)$$

Here,  $d_\theta$  is the discounted state visitation distribution defined in Section III

We provide the proof in Appendix A. Compared to offline demonstrations as guidance [28], our approach considers the human-in-the-loop setting where the agent obtains preference-labeled trajectories by interacting with the expert annotator. Therefore, although sparse rewards are unavailable for the agent in the initial training phase, LOPE can orient policy optimization by capturing more task-related information from human feedback. On the other hand, if the support sets of  $\pi$  and  $\pi_b$  are far apart or do not overlap at all, then the value of KL divergence is meaningless. In this case, the method of [28] does not work, but we provide a feasible approach to overcome the gradient vanishing problem. The entire procedure of LOPE is summarized in Algorithm 1. Hence, compared with the result of Lemma 1 in the literature [28], our result of Lemma 2 has better generalizability because of the continuity of the MMD distance.

To solve the optimization problem in Eq. (10), all that remains is to replace the expectation with sample averages, and we use the preference guidance rewards to estimate the expected returns. In this manner, existing algorithms, such as PPO or TRPO, can now easily solve the optimization problem in Eq. (8). The entire procedure of LOPE is summarized in Algorithm 1.

**Remark 1. Update Preferred Trajectory Sets with  $n$ -wise Comparisons.** Various previous work adopts the setting where the agent can only access expert preferences  $y$  for segments  $\sigma^0$  and  $\sigma^1$ . Specifically,  $y \in \{0, 0.5, 1\}$  is sampled from a discrete distribution to indicate which segment the human annotator prefers. Then, the agent records the judgment as a triple  $(\sigma^0, \sigma^1, y)$  in a data set  $\mathcal{D}$ . However, this setting cannot cover our PbRL situation with trajectory preferences.

LOPE maintains a buffer of preferred trajectories and updates this buffer with current trajectories in each iteration. Therefore, the human annotator must compare all current trajectories with the preferred trajectories in  $\mathcal{P}$  in pairs. The trajectories are ranked by human feedback, and the best  $h$  trajectories (segments) can be stored in  $\mathcal{P}$ . In practice, we set  $h = 8$  in all experiments. To achieve the  $n$ -wise comparisons, each current trajectory should be compared pair-wisely with all preference trajectories in  $\mathcal{P}$ . When the agent samples  $N$  new trajectories in each epoch, the computational complexity of  $n$ -wise comparisons is  $Nh$ . As the training progresses, the number of trajectories used to update  $\mathcal{P}$  decreases to reduce the experts' workload. The decreased number is environmentally dependent and relies on the agent's training progress.

---

**Algorithm 1** LOPE
 

---

```

1: Initialize parameters of  $\pi_\theta$ 
2: Initialize a data set of trajectory preferences  $\mathcal{P}$ 
3: for each iteration do
4:   // COLLECT TRAJECTORIES
5:   for  $k = 1, \dots, K$  do
6:     Generate batch of  $N$  trajectories  $\{\tau_i\}_i^n$  and store
       them in an on-policy buffer  $\mathcal{B}$ 
7:   end for
8:   // UPDATE POLICIES
9:   for each gradient step do
10:    Optimize the trust-region-based objective in Eq. (7)
       with respect to  $\theta$  using  $\mathcal{B}$ 
11:    Optimize the preference-guided objective in Eq. (8)
       using  $\mathcal{B}$  and  $\mathcal{P}$ 
12:   end for
13:   // UPDATE PREFERRED TRAJECTORY SETS
14:   for each trajectory in  $\mathcal{B}$  do
15:     Update preferred trajectory set  $\mathcal{P}$  with  $n$ -wise com-
       parisons
16:   end for
17: end for

```

---

## V. THEORETICAL ANALYSIS

In this section, we present the theoretical foundation of LOPE and derive a worst-case lower bound on the policy performance improvement for LOPE. We analyze the policy improvement step and preference guidance step separately. First, similar to [51], we introduce the following local approximation to  $J(\cdot)$  as follows:

$$L_\pi(\tilde{\pi}) = J(\pi) + \sum_s \rho_\pi(s) \sum_a \tilde{\pi}(a|s) A_\pi(s, a), \quad (11)$$

where  $\rho_\pi$  is the discounted state visitation distribution of  $\pi$ , and  $A_\pi$  is the advantage function of  $\pi$ . We then make the following assumption about the behavior policy  $\pi_b$  implied by the preferred trajectories in set  $\mathcal{P}$ .

**Assumption 1.**  $\pi_b$  is a **guiding** policy, and for any iteration  $k$  during training, it satisfies the following conditions:

$$\pi_b = \arg \max_{\pi} L_k(\pi), \quad (12)$$

and

$$\mathbb{E}_{a \sim \pi_b} [A_k(s, a)] \geq \Delta > 0, \quad (13)$$

where  $\rho_k$  is the discounted state visitation distribution of  $\pi_k$ , and  $L_k$  is the locally linear approximation to  $J(\cdot)$  near  $\pi_k$ .

Eq. (13) implies that the agent will produce a higher advantage by performing actions according to the demonstrations in  $\mathcal{P}$ . This is a relatively reasonable assumption since the demonstration preferred by the annotator is likely to achieve better performance than a policy that is not fully trained. It is worth mentioning that a similar assumption is adopted by [53] and [28]. However, different from these methods,  $\pi_b$  in our study is not the final optimal policy, and the expected return of  $\pi_b$  may gradually increase as an agent stores more preferred trajectories with high returns.

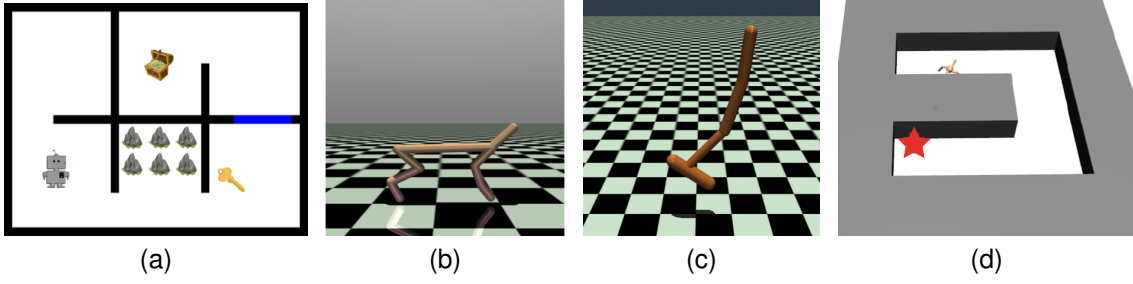


Fig. 2. The four environments for evaluating the LOPE's performance: (a) Grid World; (b) SparseHalfCheetah; (c) SparseHopper; (d) Ant Maze.

We begin with the analysis of the policy improvement step, and the following conclusion and its analysis are standard in the related literature [54].

**Proposition 1** (Performance improvement bound of the PI step [54]). *Let any policies  $\pi_k$  and  $\pi_{k+\frac{1}{2}}$  are related by Eq. (7), Then, the following bound holds:*

$$J(\pi_{k+\frac{1}{2}}) - J(\pi_k) \geq \frac{-\sqrt{2\delta}\gamma\epsilon_k}{(1-\gamma)^2}, \quad (14)$$

where  $\epsilon_k = \max_{s,a} |A_k(s,a)|$ .

We now give the following lemma to connect the difference in returns between  $\tilde{\pi}$  and  $\pi$  to the KL divergence between  $\tilde{\pi}$  and  $\pi_b$ .

**Lemma 2** (Performance improvement bound of the PG step). *For arbitrary policies  $\pi$  and  $\tilde{\pi}$ , let  $\beta = D_{\text{KL}}^{\max}(\tilde{\pi}, \pi_b) = \max_s D_{\text{KL}}(\tilde{\pi}(\cdot|s), \pi_b(\cdot|s))$ , and  $\pi_b$  is a policy satisfying Assumption 1. Then we have*

$$J(\tilde{\pi}) - J(\pi) \geq -\frac{2\beta\gamma\epsilon_b}{(1-\gamma)^2} + \frac{\Delta}{1-\gamma}, \quad (15)$$

where  $\epsilon_b = \max_{s,a} |A_b(s,a)|$  is the maximum absolute value of  $\pi_b$ 's advantage function  $A_b(s,a)$ .

The proof can be found in Appendix B.

**Remark 2.** Lemma 2 provides a quantitative description of performance improvement in the preference-guided step. The human annotator selects preferred trajectories and stores them in  $\mathcal{P}$  during training. Hence, it is reasonable to assume that  $\pi_{k+\frac{1}{2}}$  in the PG step satisfies Assumption 1 in the preference-guided step. Based on these preferred trajectories, the agent obtains a higher worst-case lower bound of performance improvement. Specifically, according to Lemma 2, for  $\pi = \pi_{k+\frac{1}{2}}$ , Eq. (15) indicates that the new lower bound increases by  $\Delta/(1-\gamma)$  than in cases where preferred trajectories are not provided.

We derive a new worst-case lower bound of LOPE's performance improvement by combining Proposition 1 and Lemma 2.

**Theorem 1** (Performance improvement bound of LOPE). *Let  $\pi_k$  and  $\pi_{k+\frac{1}{2}}$  be related by Eq. (7) and  $\pi_{k+\frac{1}{2}}$  and  $\pi_{k+1}$  be related by Eq. (8), respectively. Let  $\beta_{k+1} = D_{\text{KL}}^{\max}(\pi_{k+1}, \pi_b) =$*

$\max_s D_{\text{KL}}(\pi_{k+1}(\cdot|s), \pi_b(\cdot|s))$ . If  $\pi_{k+\frac{1}{2}}$  and  $\pi_{k+1}$  satisfies Assumption 1, then the following bound holds:

$$J(\pi_{k+1}) - J(\pi_k) \geq \frac{\Delta}{1-\gamma} - \frac{2\beta_{k+1}\gamma\epsilon_b}{(1-\gamma)^2} - \frac{\sqrt{2\delta}\gamma\epsilon_k}{(1-\gamma)^2}. \quad (16)$$

Here,  $\epsilon_k$  and  $\epsilon_b$  are as defined in Proposition 1 and Lemma 2, respectively.

We provide the proof in Appendix B. An intuitive explanation of this theorem is given in the following remark.

**Remark 3.** When the behavior policy  $\pi_b$  performs much better than the current policy as described in Assumption 1, compared to the original worst-case lower bound obtained by the TRPO algorithm, the preference-guided step results in an additional performance improvement of  $\Delta/(1-\gamma)$  size. Preference-labeled trajectories provide a more effective and accurate policy optimization direction with the agent while decreasing sampling complexity for learning. Thus, LOPE can achieve faster learning.

## VI. EXPERIMENTAL SETUPS

We evaluate LOPE on an enormous grid-world task and several continuous control tasks based on the MuJoCo physical engine [55]. The hyper-parameters used by the PyTorch code are introduced in Appendix C. In our experiments, sparse rewards are only produced by the environments, and the agent has access to both sparse rewards and human feedback.

### A. Environments

**Key-Door-Treasure domain.** As shown in Figure 2a, the Key-Door-Treasure domain is a grid-world environment similar to that defined by [7] with minor modifications. The agent should pick up the key (K) to open the door (D) and finally collect the treasure (T). The agent can only obtain a reward of 200 when reaching the treasure, and it cannot receive any rewards in other cases. The size of this grid-world environment is  $26 \times 36$ .

**Locomotion control tasks.** To explore the limitation of LOPE, we modified 2 MuJoCo tasks, HalfCheetah and Hopper, and obtained two new robots: SparseHalfCheetah and SparseHopper presented in Figs. 2b and 2c. Each of the new robots yielded a sparse reward only when the center-of-mass of the corresponding robot was beyond a certain threshold distance against the initial position, and the agent cannot be rewarded in other cases.



**Ant Maze.** To further demonstrate the feasibility of LOPE, we evaluated LOPE on an Ant-Maze task designed as a benchmark for RL by [56]. Hard exploration manifests two aspects: Locomotion and Maze. More specifically, the agent must first learn to walk and then reach the target point. The Ant is only rewarded for reaching the specified position in a maze shown in Fig. 2d. The observation space of this task is naturally decomposed into two parts: the agent’s joint angle information and task-specific attributes. The task-specific attributes include sensor readings and the positions of walls and goals.

### B. Baseline Methods

For evaluation, we compare LOPE with PEBBLE [13], the current state-of-the-art PbRL method. Additionally, our method aims to overcome exploration difficulties; therefore, NoisyNet [57] and PPO+EXP [58] are adopted as baseline methods. Meanwhile, SIL [29] and GASIL [59] are viewed as two baselines to demonstrate the LOPE’s effectiveness in exploiting previous good experiences. Lastly, we use the standard PPO [52] as a baseline method.

PEBBLE is the current state-of-the-art PbRL method. PEBBLE uses an entropy-based sampling method to improve sample and exploration efficiency. PEBBLE adopts the setting where the agent can only access expert preferences  $y$  for segments  $\sigma^0$  and  $\sigma^1$ . Specifically,  $y \in \{0, 0.5, 1\}$  is sampled from a discrete distribution to indicate which segment the human annotator prefers. Then, the agent records the judgment as a triple  $(\sigma^0, \sigma^1, y)$  in a dataset  $\mathcal{D}$ . Each time the dataset is updated, the reward model is trained to remain consistent with the preference data.

Compared with PEBBLE, the primary differences in our approach are (1) an end-to-end PbRL formulation, (2) the subtle combination of online optimization and preference guidance, and (3) the preferred set update method with  $n$ -wise comparison.

## VII. EXPERIMENTAL RESULTS

This section compares LOPE’s performance with several state-of-the-art baseline methods on extensive benchmark control tasks. These average returns were calculated over ten separate runs with different random seeds, and the shaded error bars represented the standard errors. We evaluate the agent performance quantitatively by measuring the average return computed by ground truth rewards of environments for fairness.

### A. Grid World

In the Key-Door-Treasure domain, we set the position of the key, door, and treasure room entrance as the nodes. The trajectories containing events such as picking the key, opening the door, or going through the treasure room entrance are considered preference trajectories. Moreover, trajectories closer to the goal with fewer steps are preferred. LOPE only maintains top- $h$  trajectories and leverages them to guide policy optimization, and we set  $h = 8$  in all experiments.

As shown in Fig. 3a, LOPE outperforms the other baseline methods in this grid-world task. Specifically, LOPE can learn

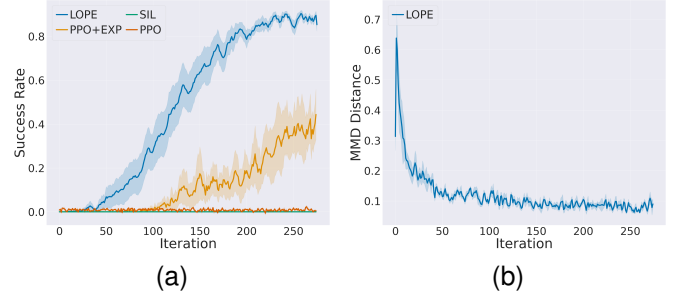


Fig. 3. (a) Learning curves of success rate in the grid-world maze; (b) Changing trend of MMD distance.

faster and achieve a higher success rate. We noted that for a long time, the baseline methods, such as PPO and SIL, could not even learn a sub-optimal policy that picks up the key and then opens the door. PPO+EXP learned faster than PPO and SIL because this algorithm could explore the environment more efficiently and find the treasure. Interestingly, LOPE learned the optimal policy most quickly. LOPE exploited preference-labeled experiences and quickly learned to open the door and further explore the broader state space. This increased the chance of obtaining the treasure reward and helped the agent learn the optimal policy during training. This instance indicates that LOPE can drive deep exploration and improve the learning efficiency of the policy with some human feedback.

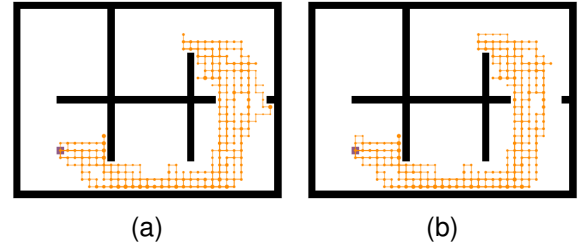


Fig. 4. (a) Actual trajectories of the learned optimal policy, (b) Preference-labeled trajectories selected by the annotator.

Fig. 3b shows the changing trend of the MMD distance between  $\pi$  and  $\pi_b$  during the training process of LOPE. Except for the later stages of the training process, a considerable MMD distance was maintained between  $\pi$  and  $\pi_b$ . Intuitively, the policy  $\pi_b$  implied by the preference data is superior to the current policy  $\pi$ . Therefore, this result demonstrates the reasonableness of Assumption 1. In this manner, updating the policy parameters towards  $\pi_b$  guarantees a higher performance improvement bound. We further depicted the actual and human-annotated trajectories in two state visitation graphs. The results are presented in Fig. 4. It implies that the agent can imitate the preference-labeled trajectories perfectly. Therefore, our method can exploit human preferences efficiently and learn the desired policy.

### B. Locomotion Tasks from MuJoCo

For easier access to preference-labeled trajectories, and notice that SparseHalfCheetah and SparseHopper can only

move along the  $x$ -axis, we set up three different nodes roughly evenly within the range of motion of the agent to determine preference-labeled trajectories. Trajectories that passed through these nodes more “gracefully” and “faster” were preferred. Specifically, the term “graceful” is used to describe that an agent can travel a greater distance at each step with less cost, that is, minimizing control costs. The term “fast” indicates that a trajectory can approach the target in fewer steps, that is, minimizing the number of steps.

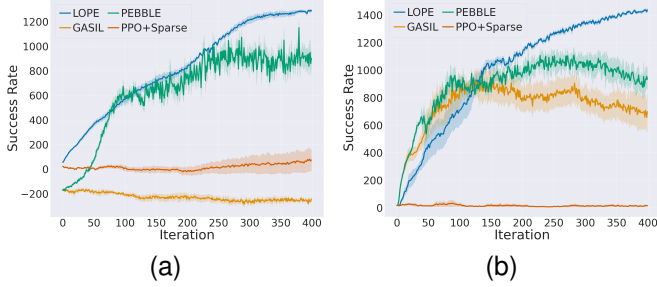


Fig. 5. Learning curves of average return on the SparseHalfCheetah and SparseHopper tasks.

As shown in Fig. 5, by selecting the preferred trajectories through the set nodes and considering them as guidance, the LOPE agent can reproduce similar behaviors quickly and gather the survival bonus in both sparse reward tasks. On the other hand, although the PEBBLE and GASIL agents exploited previous good experiences similar to our method, these methods found the optimal policy to obtain the sparse reward more slowly. They even failed to learn the optimal policy in these hard-exploration tasks. These approaches do not exploit the information in preferences, such as the agent’s coordinate position in the environment, and create remarkable information bottlenecks when utilizing previous good experiences. This information bottleneck prevents the agent from directly learning from these demonstrations. Furthermore, the PPO agent cannot perform satisfactorily on the SparseHalfCheetah and SparseHopper tasks. They depend on the action- and parameter-space noise sampled from the Gaussian distribution, which is inadequate and inefficient for hard-exploration tasks.

### C. Hard Exploration MuJoCo Maze

We set three different distance nodes and consider trajectories passing farther distance nodes as preference-labeled trajectories with higher priority in the ant-maze task. These nodes are the two corners and the target point. Trajectories that passed through these nodes more “gracefully” and “faster” were preferred. Fig. 6a presents the result.

Compared with the other baseline methods, LOPE can learn faster and achieve higher convergence values of success rate. LOPE has a solid theoretical foundation that provides a guarantee for performance improvement. Moreover, PEBBLE never received a positive reward on this challenging exploration task and did not benefit from the unsupervised pre-training and learned reward function consistent with preferences. Meanwhile, we found that SIL performed much worse than LOPE during training. This algorithm cannot

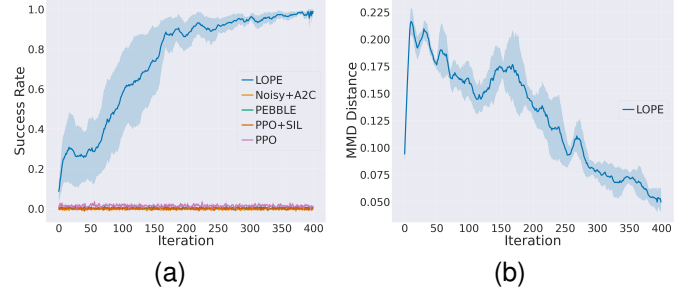


Fig. 6. (a) Learning curves of success rate on the Ant-Maze task; (b) Changing trend of MMD distance.

encounter a positive reward due to random exploration. This made it impossible to learn a good policy because there was no previous good demonstration to exploit. Furthermore, NoisyNet and PPO failed to reach the goal and learn a good policy within a reasonable time frame. This result indicates that an advanced exploration strategy is essential in hard-exploration environments for RL algorithms, and LOPE can exploit preference-labeled trajectories as guidance to drive deep exploration. Hence, our approach can avoid the potential information bottleneck and fully use data information in preferences, such as the agent’s coordination position in the environment. Fig. 6b shows the changing trend of the MMD distance between  $\pi$  and  $\pi_b$  during the training process of LOPE. The changing trend is similar to that in Fig. 3b.

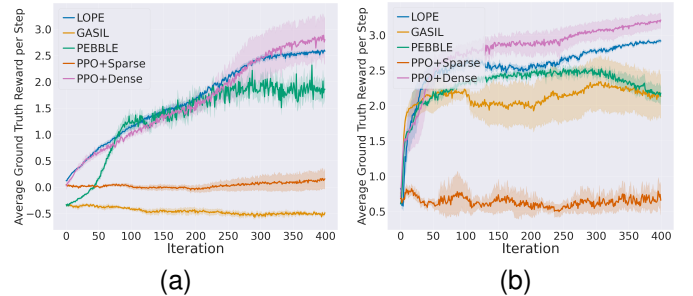


Fig. 7. Learning curves of ground-truth rewards on the SparseHalfCheetah and SparseHopper tasks.

### D. Evaluation of Ground-Truth Reward Learning

A deeper look into experimental results is provided to verify the LOPE’s effectiveness in learning near-optimal behaviors. In this experiment, we evaluated actions learned by different agents with the ground-truth reward function, which is the default setting of OpenAI Gym [60]. We then calculated the average ground-truth reward for each agent and compared them in Fig. 7. For comparison, we also trained PPO with this dense ground-truth reward function.

According to Fig. 7, the LOPE’s average ground-truth reward dramatically increases at the beginning of training, similar to PPO’s learning trend in the default OpenAI Gym reward setting. Meanwhile, the value of the LOPE’s average ground-truth reward is improved incrementally during policy optimization, and this value gradually approximates that of



PPO with the default reward function at the end of training. This result indicates that human feedback can help the agent learn near-optimal behaviors that are rewarded a high score by the default OpenAI Gym reward function.

### E. Ablation Analyses

The experimental results presented in the previous section indicate LOPE outperforms other baseline approaches on several challenging tasks. We are now interested in whether these advantages still hold when the preference setting changes. For this purpose, we designed an ablation experiment and compared the LOPE's performance on preferences with different qualities. Moreover, we conducted another ablation study on the algorithm structure to demonstrate the effectiveness of preference guidance. These ablation studies are based on the grid world environment.

**LOPE with different structures.** We ran LOPE without the policy improvement step (LOPE w/o PI) and LOPE without the preference guidance step (LOPE w/o PG) and obtained their results separately. The results are presented in Fig. 8(a). LOPE w/o PG cannot find the treasure and learn the optimal policy. In contrast, LOPE w/o PI can find the treasure; however, the learning efficiency of the optimal policy is low. This result implies that preference guidance can improve the agent's exploration efficiency while the policy improvement step guarantees the reproduction of these successful trajectories.

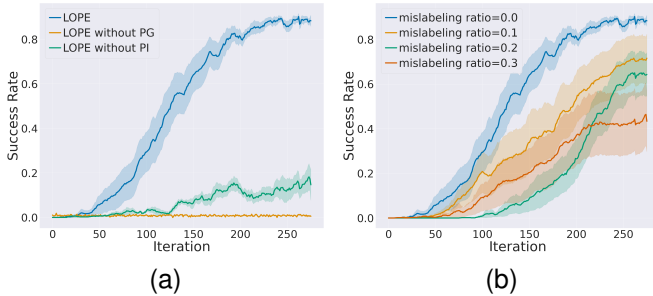


Fig. 8. Ablation results of algorithm structure and mislabeling preferences.

**Preferences with different qualities.** In this experiment, preference-labeled trajectories can be mislabeled with different ratios. Specifically, we selected four different mislabeling ratios, 0, 0.1, 0.2, 0.3, and obtained corresponding experimental results. The performance comparison is shown in Fig. 8(b). LOPE achieves the highest performance when the mislabeling ratio is 0. This result implies that the quality of demonstrations will significantly affect the performance of LOPE, and high-quality human preferences can facilitate policy optimization and accelerate learning to some extent.

## VIII. CONCLUSION

This study develops a practical PbRL algorithm for hard-exploration tasks with long horizons and sparse rewards. Our key idea is to adjust the agent's exploration by considering preferred trajectories as guidance, avoiding learning a

reward function. LOPE involves a two-step sequential policy optimization process, including trust-region-based policy improvement and preference guidance steps. Preference guidance is reformulated as a novel trajectory-wise state marginal matching problem that minimizes a novel maximum mean discrepancy distance between the preferred trajectories and the learned policy. We further provide a theoretical analysis to characterize the performance improvement bound and evaluate the effectiveness of the proposed approach. Extensive experimental results verify the superior performance of LOPE over different competitive baseline methods on several sparse-reward benchmark tasks.

### ACKNOWLEDGMENTS

This work was supported by the National Science and Technology Major Project(2022ZD0116401), the National Natural Science Foundation of China (62141605), and Fundamental Research Funds for the Central Universities.

### APPENDIX A PROOF OF LEMMA 1

**Lemma 1** (Preference guidance). *Let  $r_g(s, a)$  denote the preference guidance-based rewards, and it is expressed as:*

$$r_g(s, a) = \mathbb{E}_{\tau \in \mathcal{P}_{s,a}} [\text{dist}(\tau, \mathcal{P})]. \quad (9)$$

Here,  $\text{dist}(\tau, \mathcal{P})$  is considered the distance between  $\tau$  and  $\mathcal{P}$ , i.e.  $\text{dist}(\tau, \mathcal{P}) = \mathbb{E}_{v \sim \mathcal{P}} [d(\tau, v)]$ , and  $\mathcal{P}_{s,a} = \{\tau \in \mathcal{P} | (s, a) \in \tau\}$ . Then, Eq. (8) can be expanded as follows:

$$\begin{aligned} \pi_{k+1} &= \arg \min_{\pi_\theta} \mathbb{E}_{\substack{s \sim d_\theta \\ a \sim \pi_\theta}} [r_g(s, a)], \\ \text{s.t. } D_{\text{KL}}(\pi_\theta, \pi_{k+\frac{1}{2}}) &\leq \delta. \end{aligned} \quad (10)$$

Here,  $d_\theta$  is the discounted state visitation distribution defined in Section III

*Proof.* The objective function in Eq. (8) can be transformed as follows:

$$\mathbb{E}_{\tau \sim \rho_\theta} \left[ \mathbb{E}_{v \sim \mathcal{P}} [k(\tau, v)] \right] = \mathbb{E}_{\substack{s \sim d_\theta \\ a \sim \pi_\theta}} \left[ \mathbb{E}_{v \sim \mathcal{P}} [k(\tau, v)] \right], \quad (17)$$

where  $d_\theta$  is the discounted state visitation distribution defined in Section III.

In this manner,  $\mathbb{E}_{\tau \sim \mathcal{P}_{s,a}} [\text{dist}(\tau, \mathcal{P})]$  in Eq. (17) can be viewed as an intrinsic reward and let  $r_g(s, a) = \mathbb{E}_{\tau \sim \mathcal{P}_{s,a}} [\text{dist}(\tau, \mathcal{P})]$ . Then, we obtain

$$\mathbb{E}_{\substack{s \sim d_\theta \\ a \sim \pi_\theta}} [r_g(s, a)] = \mathbb{E}_{\tau \sim \rho_\theta} \left[ \mathbb{E}_{v \sim \mathcal{P}} [k(\tau, v)] \right]. \quad (18)$$

By substituting the original objective function in Eq. (8) with the above Eq. (18), we obtain Eq. (10). Hence, this MMD divergence minimization problem in Eq. (6) is reduced into a policy-gradient optimization algorithm with intrinsic rewards learned from human feedback. Then, the gradient of the objective function in Eq. (10) for parameters  $\theta$  is derived as follows:

$$g = \mathbb{E}_{\substack{s \sim d_\theta \\ a \sim \pi_\theta}} [\nabla_\theta \log \pi_\theta(a|s) Q_g(s, a)], \quad (19)$$

where

$$Q_g(s_t, a_t) = \mathbb{E}_{s_{t+1}, a_{t+1}, \dots} \left[ \sum_{l=0}^{\infty} \gamma^l r_g(s_{t+l}, a_{t+l}) \right]. \quad (20)$$

□

## APPENDIX B

### PROOF OF POLICY PERFORMANCE BOUND

**Definition 1** ( $\alpha$ -coupled policies [51], [53]).  $(\pi, \tilde{\pi})$  are  $\alpha$ -coupled policies if they defines a joint probability distribution  $(a, \tilde{a})|s$ , such that  $P(a \neq \tilde{a}|s) \leq \alpha$  for all  $s$ .  $\pi$  and  $\tilde{\pi}$  will denote the marginal distributions of  $a$  and  $\tilde{a}$ , respectively.

Given two arbitrary policies  $\pi_1$  and  $\pi_2$ , define the total variation discrepancy as  $D_{TV}(\pi_1, \pi_2)[s] = (1/2) \sum_a |\pi_1(a|s) - \pi_2(a|s)|$  and  $D_{TV}^{\max}(\pi_1, \pi_2) = \max_{s \in \mathcal{S}} D_{TV}(\pi_1, \pi_2)[s]$ .

**Lemma 3** (Adopted from [61]). Assume  $p_X$  and  $p_Y$  are probability distributions with  $D_{TV}(p_X, p_Y) = \alpha$ , then there exists a joint probability distribution  $(X, Y)$  whose marginal distributions are  $p_X, p_Y$ , where  $X = Y$  with probability  $1 - \alpha$ .

**Lemma 4** (Adopted from [51], [54]). Suppose  $\pi_1, \pi_2$  are two stochastic policies defined on  $\mathcal{S} \times \mathcal{A}$ , we have:

$$J(\pi_1) = J(\pi_2) + \mathbb{E}_{\tau \sim \rho_{\pi_1}} \left[ \sum_{t=0}^{\infty} \gamma^t A_{\pi_2}(s, a) \right]. \quad (21)$$

The proof details can be found in [51], and we omit them here. Given two arbitrary stochastic policies  $\pi_1$  and  $\pi_2$ , define the expected advantage of the policy  $\pi_1$  over the policy  $\pi_2$  at state  $s$  as  $A^{\pi_1|\pi_2}(s)$ :

$$A^{\pi_1|\pi_2}(s) = \mathbb{E}_{a \sim \pi_1(\cdot|s)} [A_{\pi_2}(s, a)]. \quad (22)$$

According to Lemma 4, we can derive the following conclusion. Given three arbitrary stochastic policies  $\pi, \tilde{\pi}, \pi_b$ , then the following equation holds:

$$\begin{aligned} J(\tilde{\pi}) - J(\pi_b) &= J(\pi_b) + \mathbb{E}_{\tau \sim \rho_{\tilde{\pi}}} \left[ \sum_{t=0}^{\infty} \gamma^t A^{\tilde{\pi}|\pi_b}(s_t) \right] - J(\pi_b) \\ &= \mathbb{E}_{\tau \sim \rho_{\tilde{\pi}}} \left[ \sum_{t=0}^{\infty} \gamma^t A^{\tilde{\pi}|\pi_b}(s_t) \right]. \end{aligned} \quad (23)$$

Here, Eq. (23) is obtained by defining the expected return  $J(\tilde{\pi})$  of  $\tilde{\pi}$  over  $\pi_b$  as  $J(\pi_b) + \mathbb{E}_{\tilde{\pi}} [\sum_{t=0}^{\infty} \gamma^t A^{\tilde{\pi}|\pi_b}(s_t)]$ . If we define the expected returns of  $\tilde{\pi}$  and  $\pi$  over  $\pi$ , then we have:

$$J(\tilde{\pi}) = J(\pi) + \mathbb{E}_{\tau \sim \rho_{\tilde{\pi}}} \left[ \sum_{t=0}^{\infty} \gamma^t A^{\tilde{\pi}|\pi}(s_t) \right], \quad (24)$$

$$J(\pi_b) = J(\pi) + \mathbb{E}_{\tau \sim \rho_b} \left[ \sum_{t=0}^{\infty} \gamma^t A^{\pi_b|\pi}(s_t) \right]. \quad (25)$$

Substitute Eqs. (24) and (25) into  $J(\tilde{\pi}) - J(\pi_b)$ , we have

$$\begin{aligned} J(\tilde{\pi}) - J(\pi_b) &= \mathbb{E}_{\tau \sim \rho_{\tilde{\pi}}} \left[ \sum_{t=0}^{\infty} \gamma^t A^{\tilde{\pi}|\pi}(s_t) \right] - \mathbb{E}_{\tau \sim \rho_b} \left[ \sum_{t=0}^{\infty} \gamma^t A^{\pi_b|\pi}(s_t) \right]. \end{aligned} \quad (26)$$

Combining Eqs. (23) and (26) gives

$$\begin{aligned} J(\tilde{\pi}) - J(\pi_b) &= \mathbb{E}_{\tau \sim \rho_{\tilde{\pi}}} \left[ \sum_{t=0}^{\infty} \gamma^t A^{\tilde{\pi}|\pi_b}(s_t) \right] \\ &= \mathbb{E}_{\tau \sim \rho_{\tilde{\pi}}} \left[ \sum_{t=0}^{\infty} \gamma^t A^{\tilde{\pi}|\pi}(s_t) \right] - \mathbb{E}_{\tau \sim \rho_b} \left[ \sum_{t=0}^{\infty} \gamma^t A^{\pi_b|\pi}(s_t) \right]. \end{aligned} \quad (27)$$

A similar result can be found in [53].

**Lemma 5** (Adopted from [53]). Given that  $\pi_1, \pi_2$  are  $\alpha$ -coupled policies, for any state  $s$ , then we have:

$$\left| \mathbb{E}_{s \sim \pi_1} [A^{\pi_1|\pi_2}(s)] \right| \leq 2\alpha(1 - (1 - \alpha)^t) \max_{s,a} |A_{\pi_2}(s, a)|. \quad (28)$$

The proof details of Lemma 5 can be found in [53], and we omit them here.

**Assumption 1.**  $\pi_b$  is a **guiding** policy, and for any iteration  $k$  during training, it satisfies the following conditions:

$$\pi_b = \arg \max_{\pi} L_k(\pi), \quad (12)$$

and

$$\mathbb{E}_{a \sim \pi_b} [A_k(s, a)] \geq \Delta > 0, \quad (13)$$

where  $\rho_k$  is the discounted state visitation distribution of  $\pi_k$ , and  $L_k$  is the locally linear approximation to  $J(\cdot)$  near  $\pi_k$ .

Now, we will derive the performance improvement bound described in Lemma 2. The content of Lemma 2 is described below.

**Lemma 2** (Performance improvement bound of the PG step). For arbitrary policies  $\pi$  and  $\tilde{\pi}$ , let  $\beta = D_{KL}^{\max}(\tilde{\pi}, \pi_b) = \max_s D_{KL}(\tilde{\pi}(\cdot|s), \pi_b(\cdot|s))$ , and  $\pi_b$  is a policy satisfying Assumption 1. Then we have

$$J(\tilde{\pi}) - J(\pi) \geq -\frac{2\beta\gamma\epsilon_b}{(1-\gamma)^2} + \frac{\Delta}{1-\gamma}, \quad (15)$$

where  $\epsilon_b = \max_{s,a} |A_b(s, a)|$  is the maximum absolute value of  $\pi_b$ 's advantage function  $A_b(s, a)$ .

*Proof.* Since  $\beta = D_{KL}^{\max}(\tilde{\pi}, \pi_b) = \max_s D_{KL}(\tilde{\pi}(\cdot|s), \pi_b(\cdot|s))$ , considering  $D_{TV}^2(p, q) \leq D_{KL}(p, q)$  [62], we assume  $\alpha = D_{TV}^{\max}(\tilde{\pi}, \pi_b)$  and  $\alpha$  satisfies  $\alpha^2 \leq \beta$ . According to Lemma 3,  $\pi_b, \tilde{\pi}$  are  $\alpha$ -coupled. Furthermore, it is worth mentioning that the expert policy  $\pi_b$  satisfies Assumption 1, which means

$$\mathbb{E}_{a \sim \pi_b} [A_k(s, a)] \geq \Delta > 0 \quad (29)$$

Consider introducing  $J(\pi_b)$  into  $J(\tilde{\pi})$  and  $J(\pi)$  and applying Lemma 4 to  $\tilde{\pi}$  and  $\pi_b$ , then we have

$$J(\tilde{\pi}) - J(\pi) \quad (30)$$

$$= J(\tilde{\pi}) - J(\pi_b) + J(\pi_b) - J(\pi) \quad (31)$$

$$= \mathbb{E}_{\tau \sim \rho_{\tilde{\pi}}} \left[ \sum_{t=0}^{\infty} \gamma^t A^{\tilde{\pi}|\pi}(s_t) \right] - \mathbb{E}_{\tau \sim \rho_b} \left[ \sum_{t=0}^{\infty} \gamma^t A^{\pi_b|\pi}(s_t) \right] \quad (32)$$

$$+ \mathbb{E}_{\tau \sim \rho_b} \left[ \sum_{t=0}^{\infty} \gamma^t A^{\pi_b|\pi}(s_t) \right] \quad (33)$$

TABLE I  
HYPER-PARAMETER CHOICES OF LOPE FOR DIFFERENT TASKS.

Hyper-parameter	Grid World	Ant	HalfCheetah	Hopper
Value Function Learning Rate	0.01	0.001	0.001	0.001
Policy Learning Rate	0.000015	0.00009	0.00009	0.0004
Actor Regularization	None	None	None	None
Policy Optimizer	Adam	Adam	Adam	Adam
Value Function Optimizer	Adam	Adam	Adam	Adam
Max Length per Episode	240	750	500	500
Episodes per iteration	8	30	20	20
Epochs per iteration	80	65	80	80
Discount Factor	0.99	0.99	0.99	0.99
Normalized Observations	False	False	False	False
Gradient Clipping	False	False	False	False
Initial Exploration Policy	None	$N(0, 0.17)$	$N(0, 0.15)$	$N(0, 0.65)$
Clipped Epsilon	0.3	0.21	0.2	0.27

$$= \mathbb{E}_{\tau \sim \rho_{\tilde{\pi}}} \left[ \sum_{t=0}^{\infty} \gamma^t A^{\tilde{\pi}|\pi_b}(s_t) \right] + \mathbb{E}_{\tau \sim \rho_b} \left[ \sum_{t=0}^{\infty} \gamma^t A^{\pi_b|\pi}(s_t) \right] \quad (34)$$

$$\geq - \sum_{t=0}^{\infty} \gamma^t \left| \mathbb{E}_{\tau \sim \rho_{\tilde{\pi}}} A^{\tilde{\pi}|\pi_b}(s_t) \right| + \mathbb{E}_{\tau \sim \rho_b} \left[ \sum_{t=0}^{\infty} \gamma^t A^{\pi_b|\pi}(s_t) \right] \quad (35)$$

$$\geq - \sum_{t=0}^{\infty} \gamma^t \left( 2\alpha(1 - (1 - \alpha)^t) \max_{s,a} |A_{\pi_b}(s, a) - \Delta| \right) \quad (36)$$

$$= - \frac{2\alpha^2\gamma\epsilon_b}{(1 - \gamma)(1 - \gamma(1 - \alpha))} + \frac{\Delta}{1 - \gamma} \quad (37)$$

$$\geq - \frac{2\alpha^2\gamma\epsilon_b}{(1 - \gamma)^2} + \frac{\Delta}{1 - \gamma}, \quad (38)$$

where  $\epsilon_b = \max_{s,a} |A_b(s, a)|$  is the maximum absolute value of  $\pi_b$ 's advantage function  $A_b(s, a)$ . Noting  $\beta = D_{\text{KL}}^{\max}(\tilde{\pi}, \pi_b)$  and applying  $D_{\text{TV}}^2(p, q) \leq D_{\text{KL}}(p, q)$  [62] gives

$$J(\tilde{\pi}) - J(\pi) \geq - \frac{2\beta\gamma\epsilon_b}{(1 - \gamma)^2} + \frac{\Delta}{1 - \gamma}. \quad (39)$$

Lemma 2 is proved.  $\square$

**Theorem 1** (Performance improvement bound of LOPE). *Let  $\pi_k$  and  $\pi_{k+\frac{1}{2}}$  be related by Eq. (7) and  $\pi_{k+\frac{1}{2}}$  and  $\pi_{k+1}$  be related by Eq. (8), respectively. Let  $\beta_{k+1} = D_{\text{KL}}^{\max}(\pi_{k+1}, \pi_b) = \max_s D_{\text{KL}}(\pi_{k+1}(\cdot|s), \pi_b(\cdot|s))$ . If  $\pi_{k+\frac{1}{2}}$  and  $\pi_{k+1}$  satisfies Assumption 1, then the following bound holds:*

$$J(\pi_{k+1}) - J(\pi_k) \geq \frac{\Delta}{1 - \gamma} - \frac{2\beta_{k+1}\gamma\epsilon_b}{(1 - \gamma)^2} - \frac{\sqrt{2\delta}\gamma\epsilon_k}{(1 - \gamma)^2}. \quad (16)$$

Here,  $\epsilon_k$  and  $\epsilon_b$  are as defined in Proposition 1 and Lemma 2, respectively.

*Proof.* Combining Proposition 1 and Lemma 2, we come to conclude.  $\square$

## APPENDIX C

### NEURAL NETWORK ARCHITECTURES AND HYPER-PARAMETERS

#### A. LOPE Policy Architecture for Discrete Control Tasks

(state dim, 64)  
Tanh

(64, 64)

Tanh

(64, action num)

Softmax

#### LOPE Policy Architecture for Continuous Control Tasks

(state dim, 64)

Tanh

(64, 64)

Tanh

(64, action dim)

Tanh

#### LOPE Value Function Architecture

(state dim, 64)

Tanh

(64, 64)

Tanh

(64, 1)

#### B. Hyper-parameter settings

The hyper-parameters settings are presented in Table I.

## APPENDIX D

### ADDITIONAL IMPLEMENTATION DETAILS

For clarity in the presentation, we omit certain implementation details about experiment environment settings in Section VI and describe them here. The locomotion control and ant maze tasks were implemented based on the rllab framework (<https://github.com/rll/rllab>), a framework used to develop and evaluate reinforcement learning algorithms. We ran the Hopper and HalfCheetah agents in a straight channel. Their observations consisted of the agent's joint angle information and task-specific attributes. These agents can receive sparse rewards by reaching the specified locations. We set the length of the channel to 10 units for SparseHopper and 90 units for SparseHalfCheetah. These robots were asked to move as far forward as possible. Meanwhile, the ant robot was required to walk through the E-shaped maze, as shown in Fig. 2d. This maze is a benchmark environment for hierarchical reinforcement learning [56].

## REFERENCES

- [1] V. Mnih, K. Kavukcuoglu, D. Silver, A. A. Rusu, J. Veness, M. G. Bellemare, A. Graves, M. Riedmiller, A. K. Fidjeland, G. Ostrovski *et al.*, “Human-level control through deep reinforcement learning,” *nature*, vol. 518, no. 7540, pp. 529–533, 2015.
- [2] V. Mnih, A. P. Badia, M. Mirza, A. Graves, T. Lillicrap, T. Harley, D. Silver, and K. Kavukcuoglu, “Asynchronous methods for deep reinforcement learning,” in *International conference on machine learning*. PMLR, 2016, pp. 1928–1937.
- [3] D. Silver, A. Huang, C. J. Maddison, A. Guez, L. Sifre, G. Van Den Driessche, J. Schrittwieser, I. Antonoglou, V. Panneershelvam, M. Lanctot *et al.*, “Mastering the game of go with deep neural networks and tree search,” *nature*, vol. 529, no. 7587, pp. 484–489, 2016.
- [4] H. J. Jeon, S. Milli, and A. D. Dragan, “Reward-rational (implicit) choice: A unifying formalism for reward learning,” *ArXiv*, vol. abs/2002.04833, 2020.
- [5] D. Hadfield-Menell, S. Milli, P. Abbeel, S. J. Russell, and A. D. Dragan, “Inverse reward design,” *ArXiv*, vol. abs/1711.02827, 2017.
- [6] T. Yang, H. Tang, C. Bai, J. Liu, J. Hao, Z. Meng, P. Liu, and Z. Wang, “Exploration in deep reinforcement learning: a comprehensive survey,” *arXiv preprint arXiv:2109.06668*, 2021.
- [7] Y. Guo, J. Choi, M. Moczulski, S. Feng, S. Bengio, M. Norouzi, and H. Lee, “Memory based trajectory-conditioned policies for learning from sparse rewards,” *Advances in Neural Information Processing Systems*, vol. 33, pp. 4333–4345, 2020.
- [8] C. Wirth, J. Fürnkranz, and G. Neumann, “Model-free preference-based reinforcement learning,” in *Proceedings of the AAAI Conference on Artificial Intelligence*, vol. 30, 2016.
- [9] Y. Abdelkareem, S. Shehata, and F. Karray, “Advances in preference-based reinforcement learning: A review,” in *2022 IEEE International Conference on Systems, Man, and Cybernetics (SMC)*. IEEE, 2022, pp. 2527–2532.
- [10] X. Chen, H. Zhong, Z. Yang, Z. Wang, and L. Wang, “Human-in-the-loop: Provably efficient preference-based reinforcement learning with general function approximation,” *ArXiv*, vol. abs/2205.11140, 2022.
- [11] Y. Kang, D. Shi, J. Liu, L. He, and D. Wang, “Beyond reward: Offline preference-guided policy optimization,” *arXiv preprint arXiv:2305.16217*, 2023.
- [12] P. F. Christiano, J. Leike, T. Brown, M. Martic, S. Legg, and D. Amodei, “Deep reinforcement learning from human preferences,” *Advances in neural information processing systems*, vol. 30, 2017.
- [13] K. Lee, L. Smith, and P. Abbeel, “Pebble: Feedback-efficient interactive reinforcement learning via relabeling experience and unsupervised pre-training,” *arXiv preprint arXiv:2106.05091*, 2021.
- [14] X. Liang, K. Shu, K. Lee, and P. Abbeel, “Reward uncertainty for exploration in preference-based reinforcement learning,” *arXiv preprint arXiv:2205.12401*, 2022.
- [15] C. Wirth, R. Akrou, G. Neumann, J. Fürnkranz *et al.*, “A survey of preference-based reinforcement learning methods,” *Journal of Machine Learning Research*, vol. 18, no. 136, pp. 1–46, 2017.
- [16] H. Sugiyama, T. Meguro, and Y. Minami, “Preference-learning based inverse reinforcement learning for dialog control,” in *Interspeech*, 2012.
- [17] C. Daniel, O. Kroemer, M. Viering, J. Metz, and J. Peters, “Active reward learning with a novel acquisition function,” *Autonomous Robots*, vol. 39, pp. 389–405, 2015.
- [18] L. E. Asri, B. Piot, M. Geist, R. Laroche, and O. Pietquin, “Score-based inverse reinforcement learning,” in *Adaptive Agents and Multi-Agent Systems*, 2016.
- [19] D. Arumugam, J. K. Lee, S. Saskin, and M. L. Littman, “Deep reinforcement learning from policy-dependent human feedback,” *ArXiv*, vol. abs/1902.04257, 2019.
- [20] E. R. Novoseller, Y. Sui, Y. Yue, and J. W. Burdick, “Dueling posterior sampling for preference-based reinforcement learning,” in *Conference on Uncertainty in Artificial Intelligence*, 2019.
- [21] Y. Xu, R. Wang, L. F. Yang, A. Singh, and A. W. Dubrawski, “Preference-based reinforcement learning with finite-time guarantees,” *ArXiv*, vol. abs/2006.08910, 2020.
- [22] A. Pacchiano, A. Saha, and J. Lee, “Dueling rl: Reinforcement learning with trajectory preferences,” *ArXiv*, vol. abs/2111.04850, 2021.
- [23] J. Park, Y. Seo, J. Shin, H. Lee, P. Abbeel, and K. Lee, “Surf: Semi-supervised reward learning with data augmentation for feedback-efficient preference-based reinforcement learning,” in *International Conference on Learning Representations*, 2022.
- [24] S. Schaal, “Learning from demonstration,” *Advances in neural information processing systems*, vol. 9, 1996.
- [25] T. Hester, M. Vecerik, O. Pietquin, M. Lanctot, T. Schaul, B. Piot, D. Horgan, J. Quan, A. Sendonaris, I. Osband *et al.*, “Deep q-learning from demonstrations,” in *Proceedings of the AAAI Conference on Artificial Intelligence*, 2018.
- [26] A. Rajeswaran, V. Kumar, A. Gupta, G. Vezzani, J. Schulman, E. Todorov, and S. Levine, “Learning complex dexterous manipulation with deep reinforcement learning and demonstrations,” *Robotics: Science and Systems*, 2017.
- [27] A. Nair, A. Gupta, M. Dalal, and S. Levine, “Awac: Accelerating online reinforcement learning with offline datasets,” *arXiv preprint arXiv:2006.09359*, 2020.
- [28] D. Rengarajan, G. Vaidya, A. Sarvesh, D. Kalathil, and S. Shakkottai, “Reinforcement learning with sparse rewards using guidance from offline demonstration,” in *International Conference on Learning Representations*, 2022.
- [29] J. Oh, Y. Guo, S. Singh, and H. Lee, “Self-imitation learning,” in *International Conference on Machine Learning*. PMLR, 2018, pp. 3878–3887.
- [30] T. Gangwani, Q. Liu, and J. Peng, “Learning self-imitating diverse policies,” in *7th International Conference on Learning Representations, ICLR 2019*, 2019.
- [31] G. Libardi, G. De Fabritiis, and S. Dittert, “Guided exploration with proximal policy optimization using a single demonstration,” in *International Conference on Machine Learning*. PMLR, 2021, pp. 6611–6620.
- [32] Y. Efroni, N. Merlis, and S. Mannor, “Reinforcement learning with trajectory feedback,” in *Proceedings of the AAAI Conference on Artificial Intelligence*, 2021, pp. 7288–7295.
- [33] Y. Abbasi-Yadkori, D. Pál, and C. Szepesvári, “Improved algorithms for linear stochastic bandits,” *Advances in neural information processing systems*, vol. 24, 2011.
- [34] N. Chatterji, A. Pacchiano, P. Bartlett, and M. Jordan, “On the theory of reinforcement learning with once-per-episode feedback,” *Advances in Neural Information Processing Systems*, pp. 3401–3412, 2021.
- [35] Y. Russac, L. Faury, O. Cappé, and A. Garivier, “Self-concordant analysis of generalized linear bandits with forgetting,” in *International Conference on Artificial Intelligence and Statistics*. PMLR, 2021, pp. 658–666.
- [36] M. G. Azar, I. Osband, and R. Munos, “Minimax regret bounds for reinforcement learning,” in *International Conference on Machine Learning*. PMLR, 2017, pp. 263–272.
- [37] T. Xu and Y. Liang, “Provably efficient offline reinforcement learning with trajectory-wise reward,” *arXiv preprint arXiv:2206.06426*, 2022.
- [38] R. S. Sutton and A. G. Barto, *Reinforcement learning: An introduction*. MIT press, 2018.
- [39] B. Ibarz, J. Leike, T. Pohlen, G. Irving, S. Legg, and D. Amodei, “Reward learning from human preferences and demonstrations in atari,” *Advances in neural information processing systems*, vol. 31, 2018.
- [40] N. Stiennon, L. Ouyang, J. Wu, D. Ziegler, R. Lowe, C. Voss, A. Radford, D. Amodei, and P. F. Christiano, “Learning to summarize with human feedback,” *Advances in Neural Information Processing Systems*, vol. 33, pp. 3008–3021, 2020.
- [41] J. Wu, L. Ouyang, D. M. Ziegler, N. Stiennon, R. Lowe, J. Leike, and P. Christiano, “Recursively summarizing books with human feedback,” *arXiv preprint arXiv:2109.10862*, 2021.
- [42] L. Lee, B. Eysenbach, E. Parisotto, E. Xing, S. Levine, and R. Salakhutdinov, “Efficient exploration via state marginal matching,” *arXiv preprint arXiv:1906.05274*, 2019.
- [43] S. K. S. Ghasemipour, R. Zemel, and S. Gu, “A divergence minimization perspective on imitation learning methods,” in *Conference on Robot Learning*. PMLR, 2020, pp. 1259–1277.
- [44] H. Furuta, Y. Matsuo, and S. S. Gu, “Generalized decision transformer for offline hindsight information matching,” *arXiv preprint arXiv:2111.10364*, 2021.
- [45] A. Sharma, R. Ahmad, and C. Finn, “A state-distribution matching approach to non-episodic reinforcement learning,” in *International Conference on Machine Learning*. PMLR, 2022, pp. 19 645–19 657.
- [46] I. Kostrikov, O. Nachum, and J. Tompson, “Imitation learning via off-policy distribution matching,” *arXiv preprint arXiv:1912.05032*, 2019.
- [47] A. Gretton, D. Sejdinovic, H. Strathmann, S. Balakrishnan, M. Pontil, K. Fukumizu, and B. K. Sriperumbudur, “Optimal kernel choice for large-scale two-sample tests,” *Advances in neural information processing systems*, vol. 25, 2012.
- [48] M. A. Masood and F. Doshi-Velez, “Diversity-inducing policy gradient: Using maximum mean discrepancy to find a set of diverse policies,” *arXiv preprint arXiv:1906.00088*, 2019.
- [49] G. Wang, F. Wu, and X. Zhang, “Trajectory-oriented policy optimization with sparse rewards,” *arXiv preprint arXiv:2401.02225*, 2024.

- [50] G. Wang, F. Wu, X. Zhang, and J. Liu, "Learning diverse policies with soft self-generated guidance," *International Journal of Intelligent Systems*, 2023.
- [51] J. Schulman, S. Levine, P. Abbeel, M. Jordan, and P. Moritz, "Trust region policy optimization," in *International conference on machine learning*. PMLR, 2015, pp. 1889–1897.
- [52] J. Schulman, F. Wolski, P. Dhariwal, A. Radford, and O. Klimov, "Proximal policy optimization algorithms," *arXiv preprint arXiv:1707.06347*, 2017.
- [53] B. Kang, Z. Jie, and J. Feng, "Policy optimization with demonstrations," in *International conference on machine learning*. PMLR, 2018, pp. 2469–2478.
- [54] J. Achiam, D. Held, A. Tamar, and P. Abbeel, "Constrained policy optimization," in *International conference on machine learning*. PMLR, 2017, pp. 22–31.
- [55] E. Todorov, T. Erez, and Y. Tassa, "Mujoco: A physics engine for model-based control," in *2012 IEEE/RSJ International Conference on Intelligent Robots and Systems*. IEEE, 2012, pp. 5026–5033.
- [56] Y. Duan, X. Chen, R. Houthoofd, J. Schulman, and P. Abbeel, "Benchmarking deep reinforcement learning for continuous control," in *International conference on machine learning*. PMLR, 2016, pp. 1329–1338.
- [57] M. Fortunato, M. G. Azar, B. Piot, J. Menick, I. Osband, A. Graves, V. Mnih, R. Munos, D. Hassabis, O. Pietquin *et al.*, "Noisy networks for exploration," *arXiv preprint arXiv:1706.10295*, 2017.
- [58] H. Tang, R. Houthoofd, D. Foote, A. Stooke, O. Xi Chen, Y. Duan, J. Schulman, F. DeTurck, and P. Abbeel, "# exploration: A study of count-based exploration for deep reinforcement learning," *Advances in neural information processing systems*, vol. 30, 2017.
- [59] Y. Guo, J. Oh, S. Singh, and H. Lee, "Generative adversarial self-imitation learning," *arXiv preprint arXiv:1812.00950*, 2018.
- [60] G. Brockman, V. Cheung, L. Pettersson, J. Schneider, J. Schulman, J. Tang, and W. Zaremba, "Openai gym," 2016.
- [61] D. A. Levin and Y. Peres, *Markov chains and mixing times*. American Mathematical Soc., 2017, vol. 107.
- [62] D. Pollard, "Asymptopia: an exposition of statistical asymptotic theory," URL <http://www.stat.yale.edu/pollard/Books/Asymptopia>, 2000.